A Selective Phosphatase of Regenerating Liver Phosphatase Inhibitor Suppresses Tumor Cell Anchorage-Independent Growth by a Novel Mechanism Involving p130Cas Cleavage

Sherif Daouti, Wen-hui Li, Hong Qian, Kuo-Sen Huang, Janna Holmgren, Wayne Levin, Linda Reik, Debra Lucas McGady, Paul Gillespie, Agostino Perrotta, Hongjin Bian, John F. Reidhaar-Olson, Sarah A. Bliss, Andree R. Olivier, Joseph A. Sergi, David Fry, Waleed Danho, Steve Ritland, Nader Fotouhi, David Heimbrook, and Huifeng Niu

Preclinical Research, Hoffmann-La Roche, Inc., Nutley, New Jersey

Abstract

The phosphatase of regenerating liver (PRL) family, a unique class of oncogenic phosphatases, consists of three members: PRL-1, PRL-2, and PRL-3. Aberrant overexpression of PRL-3 has been found in multiple solid tumor types. Ectopic expression of PRLs in cells induces transformation, increases mobility and invasiveness, and forms experimental metastases in mice. We have now shown that small interfering RNA–mediated depletion of PRL expression in cancer cells results in the down-regulation of p130Cas phosphorylation and expression and prevents tumor cell anchorage-independent growth in soft agar. We have also identified a small molecule, 7-amino-2-phenyl-5*H*-thieno[3,2-*c*]pyridin-4-one (thienopyridone), which potently and selectively inhibits all three PRLs but not other phosphatases *in vitro*. The thienopyridone showed significant inhibition of tumor cell anchorage-independent growth in soft agar, induction of the p130Cas cleavage, and anoikis, a type of apoptosis that can be induced by anticancer agents via disruption of cell-matrix interaction. Unlike etoposide, thienopyridone-induced p130Cas cleavage and apoptosis were not associated with increased levels of p53 and phospho-p53 (Ser^{15}), a hallmark of genotoxic drug-induced p53 pathway activation. This is the first report of a potent selective PRL inhibitor that suppresses tumor cell three-dimensional growth by a novel mechanism involving p130Cas cleavage. This study reveals a new insight into the role of PRL-3 in priming tumor progression and shows that PRL may represent an attractive target for therapeutic intervention in cancer. [Cancer Res 2008;68(4):1162–9]

Introduction

The activities of phosphatases and kinases represent a large component of the posttranslational modifications that cells use to regulate signal transduction. Phosphatases are as important as kinases; their dysregulation is known to result in neoplastic disease. The phosphatase of regenerating liver (PRL) phosphatases, a unique class of prenylated phosphatases, represent one such class with an increasing association with oncogenic and metastatic processes (1). This family of proteins consists of three closely related members, PRL-1, PRL-2, and PRL-3, which share 76% to 87% amino acid sequence identity and a unique COOH-terminal prenylation motif. Overexpression of PRL-1 or PRL-2 in epithelial cells resulted in a transformed phenotype in culture and tumor growth in nude mice (2, 3). PRL-3 was initially found amplified and overexpressed in colorectal metastatic lesions compared with normal colorectal epithelia and primary tumors (4). PRL-3 expression was elevated in nearly all metastatic samples derived from colorectal cancers regardless of the site of metastasis (liver, lung, brain, or ovary; ref. 5). Aberrant elevation of PRL-3 was also found in various other human cancers, such as liver carcinomas, gastric carcinomas, and ovarian cancers (6–8). In ovarian cancers, PRL-3 expression correlated with disease progression, being higher in advanced (stage III) than in early (stage I) tumors (8). Recent analysis of survival variables in breast cancer patients revealed shorter disease-free survival in patients with PRL-3–positive carcinomas and suggests a role of PRL-3 as a prognostic factor in breast cancer to predict worse disease outcome (9).

Furthermore, ectopic overexpression of PRL-3 in B16 cells significantly increased lung and liver metastasis compared with control cells when injected into mice. These transfectants also exhibited altered extracellular matrix adhesive properties and up-regulated integrin-mediated cell spreading efficiency (6). Additional mechanistic studies showed that PRL phosphatases promote motility and invasion by regulating the Rho family GTPase activity, the key regulators of actin cytoskeletal dynamics (10). The farnesylation of PRLs seems to be required for PRL-promoted cell invasion and motility. PRL phosphatase activity has also been shown to play an essential role in tumorigenesis. PRL-3 itself is sufficient to trigger and complete multiple steps of metastasis, whereas mutation of its catalytic domain can abolish the metastatic processes (10).

In light of the collective evidence that supports a causative role of PRL, and especially PRL-3, in tumor metastasis, targeting this class of phosphatases may provide a novel approach to cancer therapy. In the present study, we identified a selective small-molecule PRL inhibitor that suppressed tumor cell anchorage-independent growth via the induction of p130Cas cleavage and anoikis, a novel mechanism that seems independent of p53 activation.

Materials and Methods

Cancer cell lines and antibodies. Cell lines [HeLa, RKO, HT-29, MDA-MB-435, SW480, SW620, Hs688(A).T, Hs688(B).T, WM115, and WM266-4] were maintained as recommended by the distributor [American Type Culture Collection (ATCC)]. Human umbilical vascular endothelial cells (HUVEC) were obtained from Cambrex Bio Science and maintained in

Requests for reprints: Huifeng Niu, Discovery Oncology, Hoffmann-La Roche, Inc., 340 Kingsland Street, Nutley, NJ 07110. Phone: 973-235-2708; Fax: 973-235-6185; E-mail: huifeng.niu@roche.com.

doi:10.1158/0008-5472.CAN-07-2349

endothelial-specific medium EGM-2 (Cambrex Bio Science Walkersville, Inc.) according to the manufacturer's instructions.

Anti–PRL-3 antibody was purchased from R&D Systems. Pan-PRL antibody was an affinity-purified rabbit polyclonal antibody obtained from rabbits immunized with the purified keyhole limpet hemocyanin–conjugated peptide representing the COOH terminus of PRL-3 (Ac-Cys-Pro-Lys-Gln-Arg-Leu-Arg-Phe-Lys-Asp-Pro-His-Thr-His-Lys-Thr-Arg-Ser-Ser-Val-Met-OH). Additional antibodies included anti-p130Cas (BD Biosciences), anti–focal adhesion kinase (FAK; Upstate), anti–poly(ADP-ribose) polymerase (PARP; Cell Signaling Technology), anti–caspase-8 (Cell Signaling Technology), anti-p53 (Santa Cruz Biotechnology), anti–phospho-p53 (Ser^{15}; Cell Signaling Technology), and anti–β-actin (Sigma).

Western blot analysis. Cells were seeded in six-well plates 1 day before compound treatment. Upon compound treatment as indicated in the figure legends, cells were harvested and lysed immediately with 1× cell lysis buffer (Cell Signaling Technology). Protein concentrations in whole-cell extracts were determined and equal amounts of total protein (20 μg) were resolved on NuPAGE gradient gels (Invitrogen), transferred to polyvinylidene difluoride membranes, and blotted with antibodies as indicated. The protein expression was determined by densitometric quantitation of specific band intensity using Multi Gauge Software (Fujifilm).

Small interfering RNA knockdown studies. Subconfluent cells (30%) in six-well plates were transfected with 120 nmol/L nontargeting control and PRL-specific small interfering RNA (siRNA) duplexes (Dharmacon) using Lipofectamine 2000 (Invitrogen) according to the manufacturer's instructions. After transfection, cells were either seeded for soft agar assays or stimulated with 200 nmol/L phorbol 12-myristate 13-acetate (PMA) for 10 min, harvested, and subsequently analyzed by Western blot using antibodies as indicated.

Soft agar assays. RKO or HT-29 cells, grown in DMEM (90%)/fetal bovine serum (FBS; 10%) containing penicillin/streptomycin with or without siRNA transfection, were plated in DMEM (80%) containing FBS (20%), penicillin/streptomycin, and 0.3% agarose (FMC Bioproducts; top layer) in a six-well plate over DMEM (90%) containing FBS (10%), penicillin/streptomycin, and 0.5% agarose (FMC Bioproducts; bottom layer). The following day, 0.5 mL of medium with or without PRL inhibitors was added to the top layer and cells were allowed to incubate for 2 to 3 weeks.

Cloning, expression, and purification of recombinant human fusion His-PRL proteins. Full-length human fusion His_6-PRL-1 and His_6-PRL-3 cDNAs were generated by reverse transcription-PCR using either human brain (PRL-1) or human heart (PRL-3) mRNA (Clontech) as template. His_6-PRL-2 was generated from a plasmid obtained from ATCC. A hexa-His tag was incorporated at the NH_2 terminus of the forward primers. The following primers were used: His_6-PRL-1, 5′-GGAATTCCATATGCATCACCATCACCATCACGCTCGAATGAACCGCCCAGCTCCTGTGGAAGTC-3′ (forward) and 5′-CGCGGATCCTTATTGAATGCAACAGTTGTTTCTATGACC-3′ (reverse); His_6-PRL-2, 5′-GGGAATTCCATATGCATCACCATCACCATCACAACCGTCCAGCCCCTGTGGAGATCTCC-3′ (forward) and 5′-CGCGGATCCCTACTGAACACAGCAATGCCCATTGGTATC-3′ (reverse); and His_6-PRL-3, 5′-GGGAATTCCATATGCATCACCATCACCATCACGCTCGGATGAACCGCCCGGCCCCGGTGGAG-3′ (forward) and 5′-CGCGGATCCCTACATAACGCAGCACCGGGTCTTGTG-3′ (reverse). The three His_6-PRL cDNAs were cloned into the *Nde*I/*Bam*HI sites of vector pET23b (Novagen), sequenced, and expressed in *Escherichia coli*. The His_6-PRL fusion proteins were purified by binding the soluble fraction of solubilized and sonicated *E. coli* cells to Ni-NTA agarose (Qiagen) in buffer containing 25 mmol/L HEPES (pH 7.4), 300 mmol/L NaCl, 10 mmol/L imidazole, 5 mmol/L 2-mercaptoethanol, protease inhibitors, and 0.5% NP40. The bound His_6-PRL

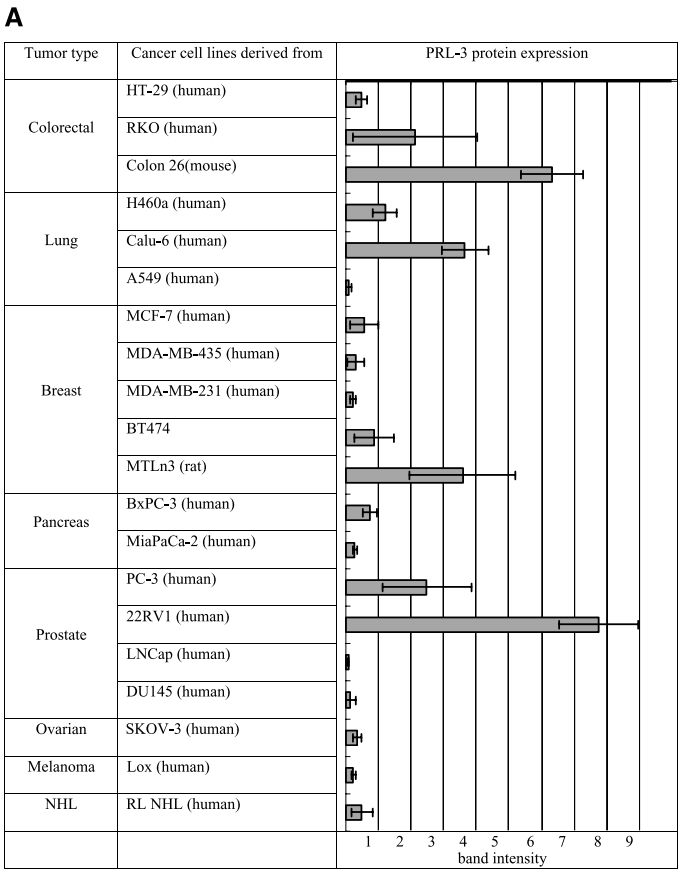

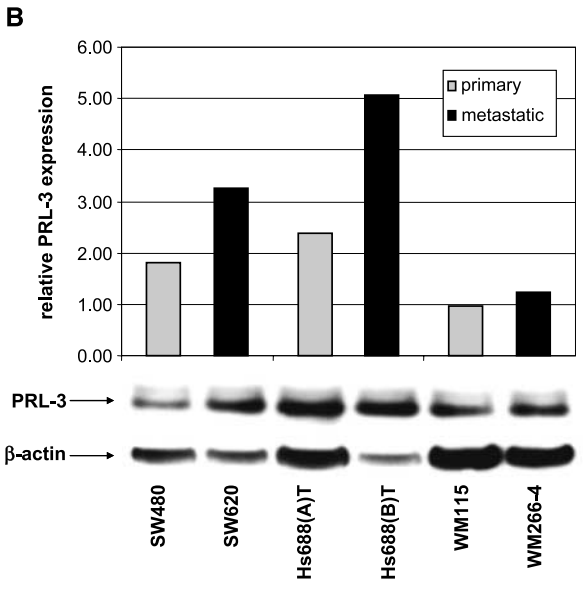

Figure 1. PRL-3 protein expression in various tumor cells. *A,* PRL-3 protein was examined by Western blot analysis of three established xenograft tumors per cancer line. The expression levels shown in the bar graph are the mean values of densitometric quantitations of PRL-3 band intensities. *B,* relative PRL-3 protein expression in three paired primary tumor and metastatic cell lines. The tumor cell lysates were analyzed by Western blot using anti–PRL-3 and anti–β-actin antibodies. The relative PRL-3 expression was quantified and normalized against β-actin levels.

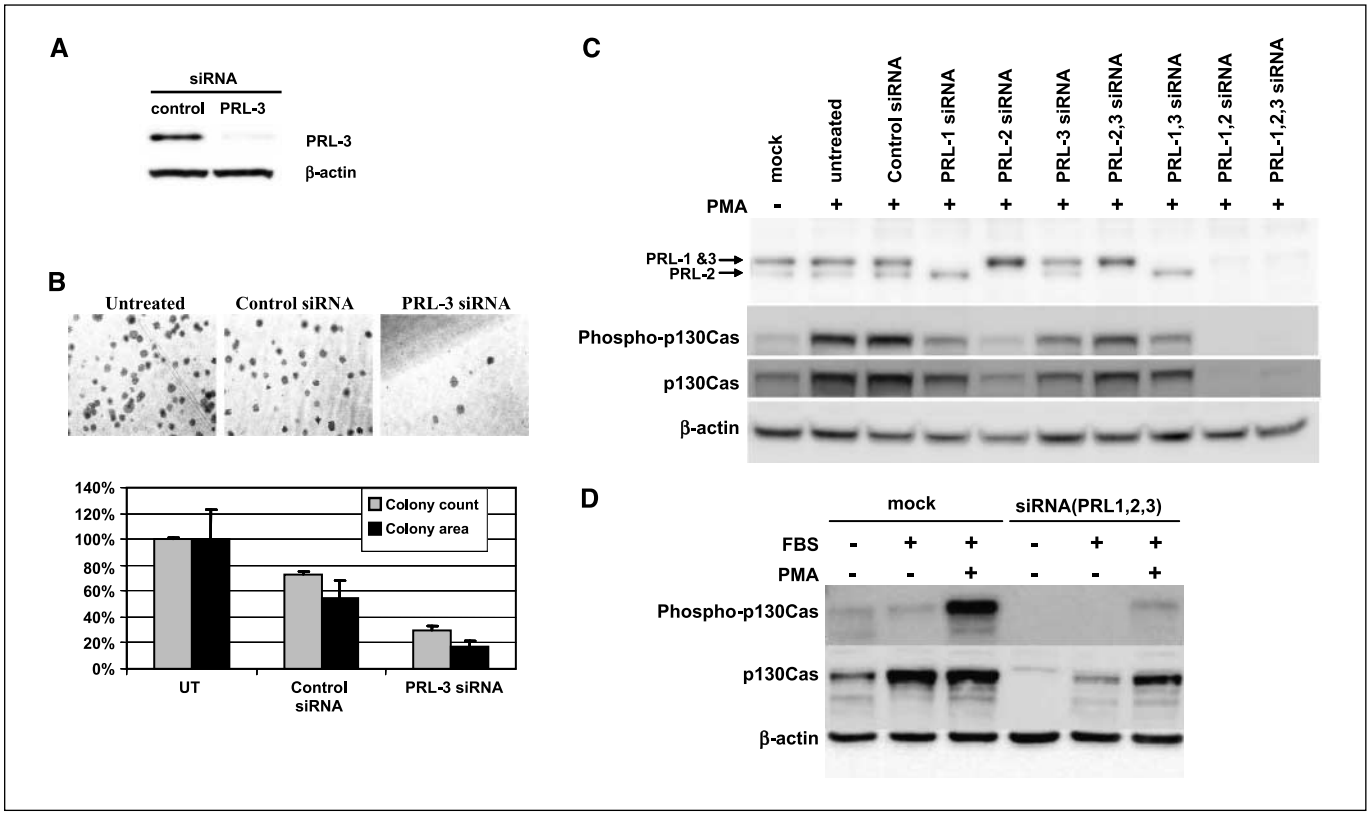

Figure 2. Cellular consequences of siRNA-mediated PRL knockdown. *A,* RKO cells were transfected with PRL-3 siRNA or control siRNA. PRL-3 protein expression was analyzed by Western blot using anti–PRL-3 antibody. β-Actin was used as a loading control. *B,* siRNA-mediated knockdown of PRL-3 prevents anchorage-independent growth of RKO cells in soft agar. At 24 h after transfection with siRNA, equal numbers of cells were mixed with soft agar and incubated at 37°C for 2 wk. *Top,* results are representative microscopic images of soft agar colonies; *bottom,* representation of three experimental measurements of colony count and area using an automatic colony reader. *UT,* untreated. *C,* siRNA-mediated knockdown of PRL results in the down-regulation of phospho-p130Cas and total p130Cas. HeLa cells were transfected with siRNA as indicated for 48 h and treated with PMA for 10 min, and cell lysates were analyzed by Western blot using pan-PRL, phospho-p130Cas, and total p130Cas antibodies as described in Materials and Methods. *D,* HeLa cells were transfected with siRNAs (against all three PRLs) for 36 h and starved in FBS-free medium overnight. FBS was added with or without PMA treatment for 10 min and phospho-p130Cas and total p130Cas were analyzed by Western blot.

proteins were eluted, concentrated, and dialyzed into a final buffer containing 20% glycerol, 20 mmol/L HEPES (pH 7.4), 100 mmol/L NaCl, 2.5 mmol/L EDTA, and 2 mmol/L DTT.

IC_{50} determination in immobilized metal ion affinity-based fluorescence polarization assays. A bead-based immobilized metal ion affinity-based fluorescence polarization (IMAP-FP) assay was performed with purified recombinant PRL proteins and peptide substrate: TAMRA-Thr-Ala-Asp-Ile-Tyr(PO3H2)-Glu-NH_2. In brief, the assay was performed in a reaction solution containing 20 mmol/L Bis-Tris (pH 6.3), 0.05% Triton X-100, and 10 mmol/L DTT in the presence of 4 μg/mL of PRL proteins, 0.5 μmol/L of TAMRA-labeled peptide substrate, and various concentrations of compounds. The highly phosphorylated peptide substrate binds to nanoparticles derivatized with trivalent metal cations through a metal-phospholigand interaction. PRL phosphatases cause a decrease in the polarization signal by removing the phosphate group. The IMAP-FP assay was performed in a 384-well plate format. The changes in fluorescence polarization were measured by a ViewLux instrument with excitation at 525 nm and emission at 598 nm.

Phosphatase selectivity assay. The phosphatase activity across a panel of phosphatases was measured as described previously (11), except that 6,8-difluoro-4-methylumbelliferylphosphate (DiFMUP; Molecular Probes) was used as substrate at the K_m for each enzyme and 10 or 37.5 mmol/L diethylglutarate (pH 6.2) was used in place of MES. The reaction was stopped with KOH and the fluorescence of the dephosphorylated substrate was measured (excitation at 360 nm/emission at 460 nm).

Cell proliferation assays. Cell viability was measured by the reduction of 3-(4,5-dimethylthiazol-2-yl)-2,5-diphenyltetrazolium bromide (MTT) to formazan. Cells were seeded in 96-well microtiter dishes and exposed to various concentrations of compounds on the following day and cultured for 5 days. After the addition of 50 μL/well of a 5 mg/mL MTT stock in Dulbecco's PBS, the cells were incubated for an additional 2.5 h at 37°C. Thereafter, the medium was removed and 50 μL of 100% ethanol were added to each well to dissolve the formazan crystals. The conversion of MTT into formazan by viable cells was assessed by a microplate reader at 570 nm. HUVEC viability was assessed by the reduction of Alamar Blue, which was measured spectrophotometrically. The procedure was done in accordance with the manufacturer's instructions (BioSource International, Inc.).

Cell migration assay. HUVEC migration was measured using a real-time cell invasion and migration (RT-CIM) assay system (ACEA Biosciences, Inc.). Cells (4×10^4) were seeded in the upper chamber in basal medium containing 0.1% bovine serum albumin in the presence of DMSO or various concentrations of compound. The lower chamber contained complete HUVEC medium (EGM-2) with growth factors and additives. Cell migration was monitored every 10 min for a period of 24 h.

Results

PRL-3 expression in human xenograft tumors. PRL-3 mRNA levels have been reported in various cancer cells. To further examine the protein expression levels of PRL-3 in cancer cells in a tumor environment, we excised established human xenograft tumors derived from 20 different cancer lines in nude mice and analyzed the tumor tissue lysates by Western blot analysis using

anti–PRL-3 antibody. Screening results shown in Fig. 1*A* indicate that PRL-3 protein expression varies among different tumor lines without a clear correlation with tumor type or with any genetic alterations, such as p53 mutation. It is worth noting that high levels of PRL-3 protein were found in rat mammary adenocarcinoma MTLn3, a lung metastasis-derived subclone line with high metastatic potential (12). We further analyzed PRL-3 protein expression in three paired primary and metastatic tumor lines, where each pair is derived from the same patient: (*a*) SW480 (primary colorectal cancer) and SW620 (metastasis), (*b*) Hs688(A).T (primary melanoma) and Hs688(B).T (metastasis), and (*c*) WM115 (primary melanoma) and WM266-4 (metastasis). As shown in Fig. 1*B*, relatively high levels of PRL-3 expression were confirmed in two metastatic lines compared with their respective primary lines.

Cellular consequences of PRL knockdown using siRNA. The exact biological function of PRL is poorly understood, and a specific PRL substrate has not been identified thus far. To investigate the cellular consequences of PRL inhibition, we examined the effect of PRL-3 knockdown on cell proliferation in two-dimensional and three-dimensional culture conditions. In MTT assays of various cancer cells under normal two-dimensional culture condition, there were minimal changes in viability in cells transfected with PRL siRNA or control siRNA (data not shown). Considering the tight association of PRL-3 with cancer metastasis, we performed soft agar assays to examine whether PRL-3 knockdown has an effect on cell growth under three-dimensional culture condition. The human colorectal cell line RKO was chosen because it expresses PRL-3 and forms uniform colonies in soft agar. After transfection of PRL-3 siRNA or control siRNA for 24 h, RKO cells were plated in soft agar and grown for 2 weeks. PRL-3 protein expression in RKO cells was shown to be specifically abolished by siRNA (Fig. 2*A*). The depletion of PRL-3 further led to the inhibition of anchorage-independent cell growth in soft agar as shown in the top panel (representative images) and the bottom panel (quantitative summary) of Fig. 2*B*. These results agree with previous reports that specific knockdown of PRL-3 in cancer cells prevents their migration and invasion but not proliferation (13, 14). To gain insight into the mechanistic role of PRL, we systematically profiled the expression of various proteins in cancer cells following knockdown of each individual PRL or a combination of two/three PRLs. We focused our evaluation primarily on those well-known proteins implicated in cell migration and invasion. As shown in Fig. 2*C* (*top*), PRL expression was completely knocked down by transfection of respective siRNA in HeLa cells. The differential depletion patterns of PRL protein expression in cells suggest that HeLa cells express high levels of PRL-1 and PRL-2 but hardly any PRL-3. Interestingly, we found that down-regulation of phosphorylated and total p130Cas levels was associated with PRL knockdown and was more prominent in cells transfected with all three PRL siRNAs (Fig. 2*C*, *middle*), whereas the amount of control protein β-actin remained constant (Fig. 2*C*, *bottom*). These results identify a functional link between PRL and p130Cas and suggest a role for PRL in regulating p130Cas phosphorylation and expression. Because p130Cas signaling is a target of many exogenous stimuli, we further measured phospho-p130Cas and total p130Cas levels in response to serum (FBS) and PMA stimulation in cells with or without PRL knockdown. As shown in Fig. 2*D*, increased levels of phospho-p130Cas were observed in controls in response to PMA stimulus and total p130Cas was induced by either FBS or PMA. Following transfection of PRL siRNAs (PRL-1, PRL-2, and PRL-3), the FBS- and PMA-induced elevation of phospho-p130Cas and total p130Cas was significantly suppressed. Our results reveal a functional role of PRL in the regulation of exogenous growth/survival signaling-induced p130Cas pathway activation, which may in turn contribute to a provocative role in cell migration, invasion, and metastasis.

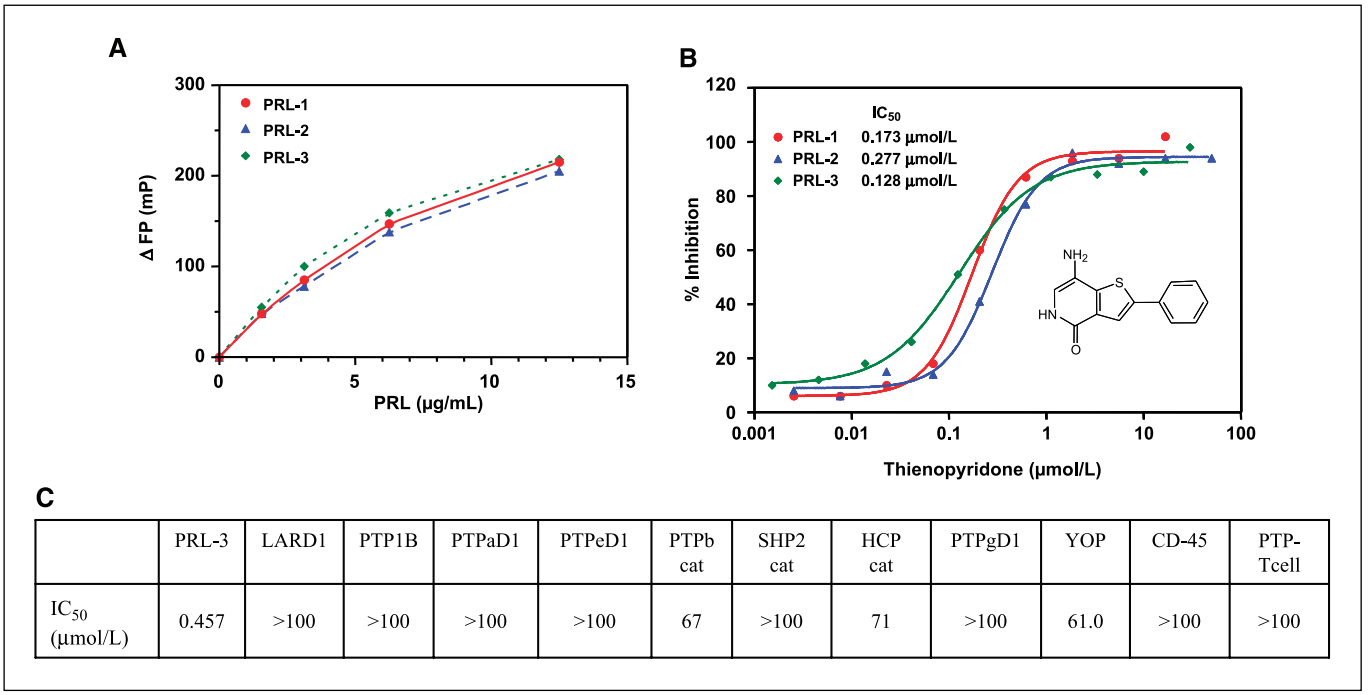

C

	PRL-3	LARD1	PTP1B	PTPaD1	PTPeD1	PTPb cat	SHP2 cat	HCP cat	PTPgD1	YOP	CD-45	PTP-Tcell
IC_{50} (μmol/L)	0.457	>100	>100	>100	>100	67	>100	71	>100	61.0	>100	>100

Figure 3. Identification of the thienopyridone as a potent selective PRL inhibitor. *A,* concentration-dependent PRL phosphatase activities in IMAP-FP assays. *ΔFP(mP),* fluorescence polarization (millipolarization unit) change. *B,* chemical structure and IC_{50} of a potent PRL inhibitor (thienopyridone) against all three PRL enzymes in IMAP-FP assays. *C,* selectivity assays of the thienopyridone against PRL-3 and 11 other phosphatases using DiFMUP as a substrate.

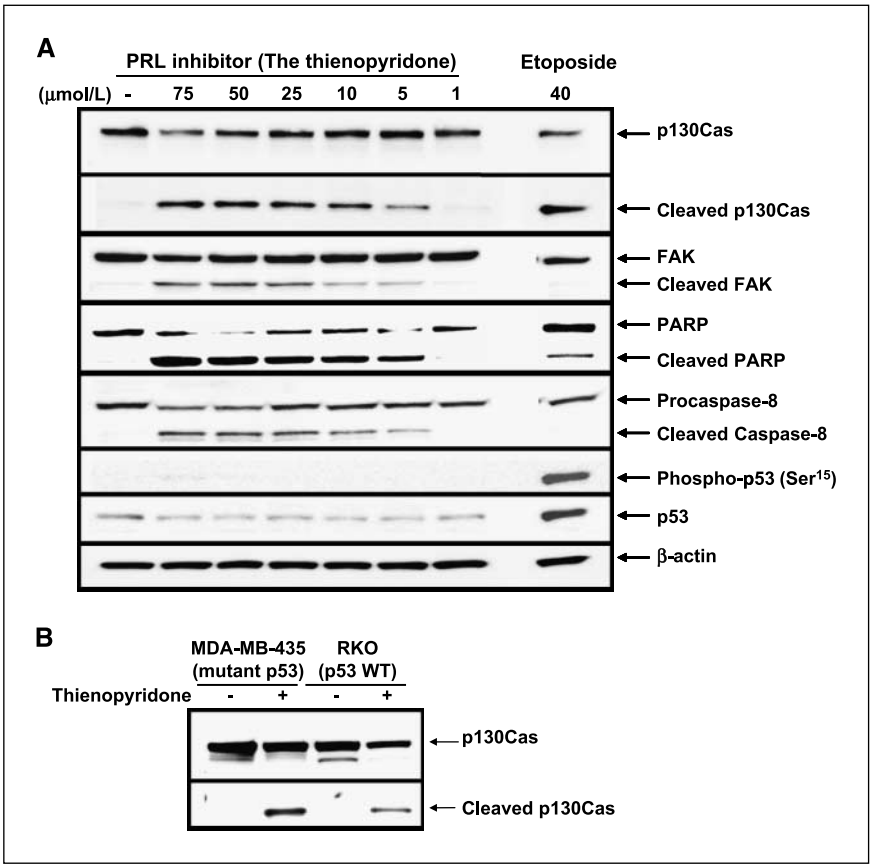

Figure 4. Mechanistic action of the thienopyridone in cancer cells. *A,* induction of proteolytic cleavage of p130Cas and apoptosis in cancer cells by the thienopyridone. HeLa cells were treated with various concentrations of the thienopyridone or etoposide for 24 h; the cellular extracts were analyzed by Western blot using antibodies against p130Cas, FAK, caspase-8, phospho-p53 (Ser^{15}), p53, and β-actin as indicated. *B,* the thienopyridone induced proteolytic cleavage of p130Cas independent of p53 mutation status in cancer cells. Human breast cancer cell line MDA-MB-435 (mutant p53) and human colorectal cancer cell line RKO (WT p53) were treated with the thienopyridone for 24 h. The cell lysates were analyzed by Western blot using anti-p130Cas antibodies.

Identification of PRL inhibitor. Targeting PRL may be a useful strategy to hinder cancer cell invasion and metastasis. To identify PRL inhibitors, we established a high-throughput IMAP-FP screening assay using purified recombinant PRL proteins. Using the same peptide as the substrates, the concentration-dependent changes in fluorescence polarization in assays showed that all three PRL proteins have similar phosphatase activities (Fig. 3*A*). By screening the Roche chemical library, positive hits were identified by compound-induced reduction in fluorescence. Our primary screen revealed a class of fused pyridone molecules as potent reversible PRL inhibitors. The structure and activities of a selected compound, 7-amino-2-phenyl-5*H*-thieno[3,2-*c*]pyridin-4-one, referred to as the thienopyridone, are shown in Fig. 3*B*. It exhibited similar IC_{50} values of 0.173, 0.277, and 0.128 μmol/L in PRL-1, PRL-2, and PRL-3 phosphatase assays, respectively. To examine its selectivity, we further examined activities of the thienopyridone in a phosphatase assay panel of 11 other phosphatases representing different classes of phosphatases, including tyrosine and dual-specific phosphatases. As shown in Fig. 3*C*, using DiFMUP as a substrate for all protein phosphatase (PTPase) assays, the thienopyridone displayed excellent selectivity against PRL-3 phosphatase with an IC_{50} of 0.457 μmol/L, but showed minimal effects on other phosphatases.

Effects of PRL inhibitor on tumor cells and the mechanism of action. After revealing specific cellular consequences of PRL depletion using siRNA, we next examined the cellular effects of the PRL inhibitor. A dose-dependent down-regulation of total p130Cas was observed in HeLa cells treated with the thienopyridone PRL inhibitor (Fig. 4*A, row 1*). Although the compound effect was not as significant as that induced by PRL siRNAs, we found that the thienopyridone induced a specific cleavage fragment recognized by anti-p130Cas antibody (Fig. 4*A, row 2*). It has been reported that proteolysis of p130Cas is associated with the induction of apoptosis by different agents (etoposide, cisplatin, and celecoxib) and generates a 31-kDa fragment (15, 16). This small fragment is translocated to the nucleus where it acts as a transcriptional repressor and leads to anoikis, a type of apoptosis caused by disruption of cell-matrix interactions (17). To determine whether the PRL inhibitor induced the same proteolysis of p130Cas, HeLa cells were treated with the thienopyridone or with etoposide as a control, and the cell extracts were run side by side. As shown in Fig. 4*A* (*rows 1* and *2*), both the thienopyridone and etoposide induced p130Cas cleavage and generated fragments that were aligned at the same position on SDS-PAGE. Because the proteolysis of p130Cas is associated with the onset of anoikis, we then examined the possible cleavage of other components of the focal adhesion complexes. We found that FAK was also cleaved by the thienopyridone PRL inhibitor, whereas etoposide only induced minimal FAK cleavage, suggesting different kinetics from the p130Cas cleavage (Fig. 4*A, row 3*). Furthermore, thienopyridone-induced p130Cas and FAK cleavage led to caspase-mediated cell apoptosis as evidenced by the simultaneous induction of the cleavage of PARP and caspase-8 (Fig. 4*A, rows 4* and *5*). Etoposide-induced apoptosis involved minimal caspase-8 cleavage consistent with a previous report (15). Most genotoxic drugs, such as etoposide, are well known to trigger cell death by inducing DNA damage and p53 pathway activation. To further understand whether the PRL inhibitor has the same mechanism of action, we then assessed the effects of both

compounds on the p53 pathway. Our results showed that etoposide but not the thienopyridone induced a posttranslational increase in p53 levels, especially in phospho-p53 (Ser^{15}) levels, a hallmark of DNA-damaging agent-induced p53 pathway activation (Fig. 4*A, rows 6* and *7*). In addition, thienopyridone-induced proteolysis of p130Cas was detected in MDA-MB-435 breast cancer line (mutant p53) and RKO colorectal cancer line [wild-type (WT) p53] independent of the p53 gene mutation status (Fig. 4*B*). Together, these results suggest that the PRL inhibitor induces p130Cas cleavage and apoptosis via a novel mechanism that seems independent of p53 activity and is distinct from other anticancer drugs.

Next, we examined the effect of the thienopyridone on cancer cell anchorage-independent growth. The human colorectal cancer cells RKO and HT-29 express PRL-3 and form uniform colonies in soft agar. After 2 weeks of culture in medium with or without various concentrations of the thienopyridone, control (DMSO-treated) cells formed many colonies in soft agar, whereas the thienopyridone-treated cells (both RKO and HT-29 cells) had significant reduction in colony formation (Fig. 5*A*). The PRL inhibitor exhibited a dose-dependent inhibition in cancer cell anchorage-independent growth as measured by either colony number or colony size (Fig. 5*B*). The EC_{50} values of the thienopyridone were 3.29 and 3.05 μmol/L for RKO and HT-29 cells, respectively (Fig. 5*A* and *B*).

Effects of PRL inhibitors on HUVECs. Several published results have shown a role for PRL-3 in both endothelial and malignant cells (6, 13). PRL-3 mRNA has been detected in a subset of endothelial cells in human colon samples (4). Basal level of PRL-3 mRNA is low in endothelial cells but can be increased upon PMA exposure (13). We confirmed the expression of PRL-3 protein in

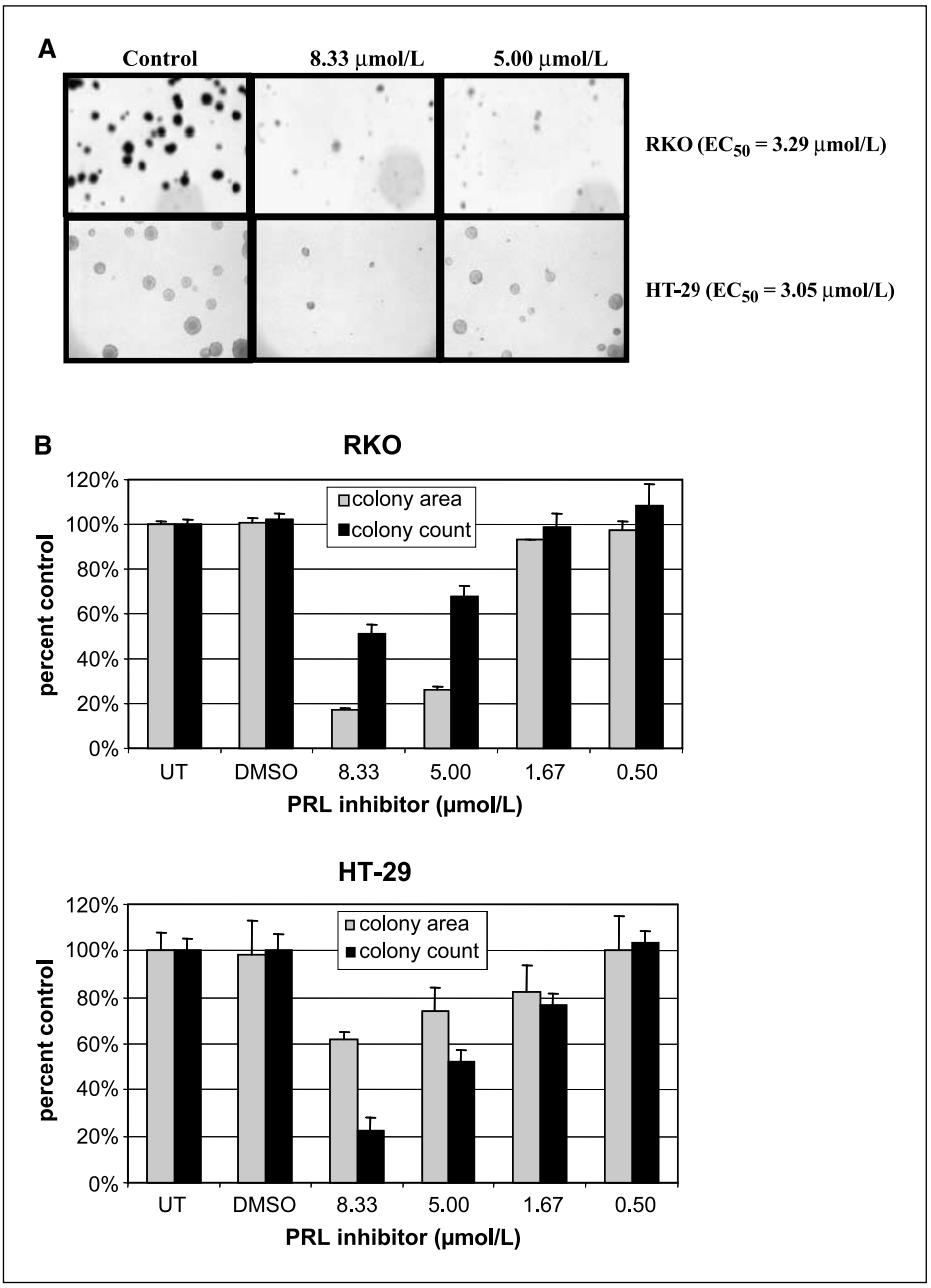

Figure 5. The PRL inhibitor prevents anchorage-independent tumor cell growth in soft agar. RKO and HT-29 colorectal cancer cells were grown in soft agar in the presence or absence of various concentrations of the thienopyridone. *A,* representative images of cell colonies grown in soft agar. EC_{50} of the thienopyridone was calculated based on the measurement of colony count or colony area. *B,* representative bar graphs of colony area and colony count for cells grown in soft agar (measured by an automated colony reader). The results were derived from triplicates of each assay sample.

HUVECs and its up-regulation upon mitogen (PMA) stimulation (Fig. 6*A*). Because PMA-stimulated HUVECs have shown increased cell proliferation, cell invasion, and tube formation, which correlates with high levels of PRL-3 expression (13), we tested the effect of thienopyridone on HUVEC migration and proliferation. HUVEC migration and viability were examined by the RT-CIM assay system and the Alamar Blue assay, respectively. As the results in Fig. 6*B* show, the thienopyridone PRL inhibitor significantly suppressed HUVEC migration but not proliferation when measured at the same time point after compound treatment. This result suggests a potential role for PRL inhibitors in targeting both endothelial and tumor cells. A PRL inhibitor may serve as a therapeutic agent to simultaneously inhibit tumor angiogenesis and anchorage-independent tumor cell growth.

Discussion

Dysregulation and clinical correlation of PRL protein expression suggest a role for PRL in cancer invasion and metastasis. However, the detailed mechanism remains largely unknown. By using PRL siRNA and a small molecular PRL inhibitor, we specifically abolished PRL expression or inhibited PRL activities in tumor cells, which in parallel reveal a novel mechanistic link of PRL with the p130Cas signaling pathway. p130Cas is a well-known adaptor protein involved in cellular functions, such as survival, proliferation, and migration, and is therefore important in pathologic processes, such as tumorigenesis and invasion (18). Cas was initially identified as a major tyrosine-phosphorylated substrate of the oncogenes v-Crk and v-Src. Many growth factors and hormones also regulate p130Cas tyrosine phosphorylation. Increased p130Cas phosphorylation is associated with cell motility and invasion (19). Src-induced oncogenic transformation is associated with many dramatic changes in cell morphology, actin organization, and anchorage independence. p130Cas is an essential cofactor involved in the Src-induced oncogenic process, as p130Cas-null cells cannot be transformed by Src and are unable to grow in soft agar. Even without Src transformation, p130Cas-null cells show defects in cell spreading, actin bundling, and cell migration. We hypothesize that PRL phosphatases might regulate the p130Cas signaling pathway, which in turn leads to a promoting role in tumor metastasis. Interestingly, PRL phosphatases have been found to stimulate the Rho signaling pathway (10), and Rho family GTPases are also critical regulators of actin organization associated with cell motility and cell cycle progression. It is worth exploring further the connective relationship between these molecules to better understand the exact signaling networks among PRL, Src, Cas, and Rho that are critical for tumor migration and invasion.

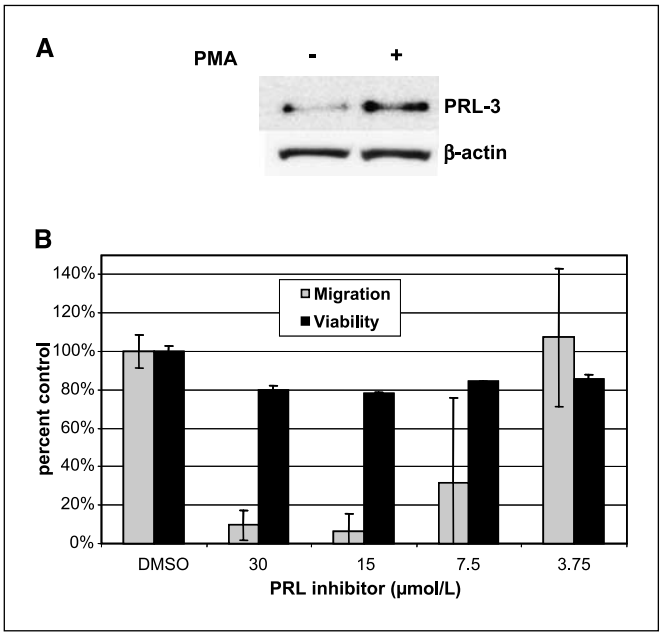

Figure 6. The thienopyridone dose dependently inhibits HUVEC migration but not proliferation. *A,* HUVECs were treated with control (DMSO) or 100 nmol/L PMA for 24 h; the cell lysates were resolved on SDS-PAGE and analyzed by Western blot using anti–PRL-3 and anti–β-actin antibodies. *B,* HUVEC migration was assessed by the RT-CIM assay system as described in Materials and Methods. Results shown are the end-point analysis of the migrated cells after 24 h of compound treatment. In parallel, HUVEC viability was determined by the Alamar Blue assay at the same time point.

There is a close correlation between p130Cas cleavage and anoikis (20). Multiple proapoptotic stimuli, such as anticancer agent etoposide or cisplatin treatment, induce p130Cas cleavage to generate a small 31-kDa fragment. This fragment is sufficient to initiate anoikis and induce cell death. Constitutive phosphorylation of p130Cas results in resistance to anoikis, leading to anchorage-independent tumor growth and metastasis. The present study shows that p130Cas phosphorylation and expression can be down-regulated in cells depleted of PRL. A recent report also shows that PRL-1 knockdown decreased c-Src and p130Cas expression in human lung cancer cells (21). The correlative expression found for PRL and p130Cas suggests a role of PRL in the regulation of p130Cas phosphorylation and expression. This is further supported by the fact that the thienopyridone, a specific PRL inhibitor, induced p130Cas cleavage, generated the same 31-kDa fragment, and induced cell death. Unlike other anticancer drugs, PRL inhibitor-induced p130Cas cleavage and cellular apoptosis seem to be independent of p53 pathway activation. Interestingly, the p130Cas cleavage was not observed in tumor cells in which all PRLs were knocked down using siRNA. This is not unexpected. Notably, PRL is a prenylated PTPase and prenylation is required for the subcellular localization and full biological function of the protein. Thus, the cellular consequences of PRL depletion may not be completely identical to that of the inhibition of the phosphatase activity of PRL by a small-molecule inhibitor. It is intriguing that the PRL inhibitor did not induce p130Cas cleavage in three normal cells, including Detroit 551 normal fibroblasts from skin, MR-90 normal fibroblasts from lung, and FHs 74 Int normal epithelial cells from small intestine (data not shown), which may imply that normal cells have a better apoptotic protective mechanism than cancer cells. Indeed, the thienopyridone had minimal nonspecific cytotoxic effects on these normal cells, as the EC_{90} values are all above 30 μmol/L in MTT assays (data not shown). In addition, the thienopyridone has no effect on HUVEC proliferation (Fig. 6*B*). Because cancer deaths mainly result from tumor metastasis rather than from primary tumors, our results suggest that a specific PRL inhibitor may provide alternative clinical benefit in the treatment of human cancer by affecting tumor migration and invasion via a novel mechanistic action in regulating p130Cas expression.

To validate whether PRL represents a novel anticancer target, we initiated discovery efforts to identify a potent selective inhibitor. A group of fused pyridone compounds was revealed by high-throughput screening. Some of these compounds seemed to inhibit the phosphatase activities by a redox mechanism via

generation of a reactive oxygen species, which causes the cyclization of DTT. However, several compelling lines of evidence suggest that inhibition of PRLs by the thienopyridone is not due to a redox mechanism. First, adding the thienopyridone to PRL-3 in a nuclear magnetic resonance experiment did not lead to the appearance of peaks consistent with the oxidized form of PRL-3 (22), although it was able to oxidize DTT *in vitro* (data not shown). Second, the thienopyridone possessed excellent selectivity inhibiting PRL but not 11 other phosphatases, which represent different classes of phosphatase with diverse sequence, structure, and function (Fig. 3*C*). Third, the thienopyridone had minimal nonspecific cytotoxic effects on normal cells, including HUVEC (Fig. 6*B*). Fourth, similar to siRNA-mediated PRL knockdown effect in tumor cells, the thienopyridone also regulated p130Cas expression and suppressed tumor cell anchorage-independent growth (Figs. 2, 4, and 5). Fifth, the thienopyridone-induced cell apoptosis was not associated with the DNA damage-induced p53 pathway activation that could be caused by a redox compound (Fig. 4).

Despite the increasing evidence *in vitro* that suggests a causative role of PRL in human cancers, the *in vivo* relevance of PRL in tumorigenesis is not yet clear. *In vivo* knockout mice may further define PRL function; however, there may be limitations in determining its role in adulthood. A specific PRL inhibitor provides a valuable tool to explore the regulatory connection between PRL and Src, p130Cas, Rho, and other downstream target genes. To ultimately show the development potential for a specific PRL inhibitor as a novel anticancer agent, further extensive work on the thienopyridone would be required due to concern about risks associated with redox activity, although no evidence of any selectivity or safety issues has been found *in vitro*.

Acknowledgments

Received 6/22/2007; revised 11/30/2007; accepted 12/19/2007.

The costs of publication of this article were defrayed in part by the payment of page charges. This article must therefore be hereby marked *advertisement* in accordance with 18 U.S.C. Section 1734 solely to indicate this fact.

We thank John Boylan for discussions and critical evaluation of the manuscript and Huisheng Wang for technical assistance.

References

1. Stephens BJ, Han H, Gokhale V, Von Hoff DD. PRL phosphatases as potential molecular targets in cancer. Mol Cancer Ther 2005;4:1653–61.
2. Cates CA, Michael RL, Stayrook KR, et al. Prenylation of oncogenic human PTP(CAAX) protein tyrosine phosphatases. Cancer Lett 1996;110:49–55.
3. Wang Q, Holmes DI, Powell SM, Lu QL, Waxman J. Analysis of stromal-epithelial interactions in prostate cancer identifies PTPCAAX2 as a potential oncogene. Cancer Lett 2002;175:63–9.
4. Saha S, Bardelli A, Buckhaults P, et al. A phosphatase associated with metastasis of colorectal cancer. Science 2001;294:1343–6.
5. Bardelli A, Saha S, Sager JA, et al. PRL-3 expression in metastatic cancers. Clin Cancer Res 2003;9:5607–15.
6. Wu X, Zeng H, Zhang X, et al. Phosphatase of regenerating liver-3 promotes motility and metastasis of mouse melanoma cells. Am J Pathol 2004;164:2039–54.
7. Miskad UA, Semba S, Kato H, et al. High PRL-3 expression in human gastric cancer is a marker of metastasis and grades of malignancies: an *in situ* hybridization study. Virchows Arch 2007;450:303–10.
8. Polato F, Codegoni A, Fruscio R, et al. PRL-3 phosphatase is implicated in ovarian cancer growth. Clin Cancer Res 2005;11:6835–9.
9. Radke I, Gotte M, Kersting C, Mattsson B, Kiesel L, Wulfing P. Expression and prognostic impact of the protein tyrosine phosphatases PRL-1, PRL-2, and PRL-3 in breast cancer. Br J Cancer 2006;95:347–54.
10. Fiordalisi JJ, Keller PJ, Cox AD. PRL tyrosine phosphatases regulate Rho family GTPases to promote invasion and motility. Cancer Res 2006;66:3153–61.
11. Guertin KR, Setti L, Qi L, et al. Identification of a novel class of orally active pyrimido[5,4-3][1,2,4]triazine-5,7-diamine-based hypoglycemic agents with protein tyrosine phosphatase inhibitory activity. Bioorg Med Chem Lett 2003;13:2895–8.
12. Neri A, Welch D, Kawaguchi T, Nicolson GL. Development and biologic properties of malignant cell sublines and clones of a spontaneously metastasizing rat mammary adenocarcinoma. J Natl Cancer Inst 1982;68:507–17.
13. Rouleau C, Roy A, St. Martin T, et al. Protein tyrosine phosphatase PRL-3 in malignant cells and endothelial cells: expression and function. Mol Cancer Ther 2006;5:219–29.
14. Kato H, Semba S, Miskad UA, Seo Y, Kasuga M, Yokozaki H. High expression of PRL-3 promotes cancer cell motility and liver metastasis in human colorectal cancer: a predictive molecular marker of metachronous liver and lung metastases. Clin Cancer Res 2004;10:7318–28.
15. Kook S, Shim SR, Choi SJ, et al. Caspase-mediated cleavage of p130cas in etoposide-induced apoptotic Rat-1 cells. Mol Biol Cell 2000;11:929–39.
16. Casanova I, Parreno M, Farre L, et al. Celecoxib induces anoikis in human colon carcinoma cells associated with the deregulation of focal adhesions and nuclear translocation of p130Cas. Int J Cancer 2006;118:2381–9.
17. Kim W, Kook S, Kim DJ, Teodorof C, Song WK. The 31-kDa caspase-generated cleavage product of p130cas functions as a transcriptional repressor of E2A in apoptotic cells. J Biol Chem 2004;279:8333–42.
18. Cabodi S, Tinnirello A, Di Stefano P, et al. p130Cas as a new regulator of mammary epithelial cell proliferation, survival, and HER2-neu oncogene-dependent breast tumorigenesis. Cancer Res 2006;66:4672–80.
19. Defilippi P, Di Stefano P, Cabodi S. p130Cas: a versatile scaffold in signaling networks. Trends Cell Biol 2006;16:257–63.
20. Wei L, Yang Y, Zhang X, Yu Q. Cleavage of p130Cas in anoikis. J Cell Biochem 2004;91:325–35.
21. Achiwa H, Lazo JS. PRL-1 tyrosine phosphatase regulates c-Src levels, adherence, and invasion in human lung cancer cells. Cancer Res 2007;67:643–50.
22. Kozlov G, Cheng J, Ziomek E, Banville D, Gehring K, Ekiel I. Structural insights into molecular function of the metastasis-associated phosphatase PRL-3. J Biol Chem 2004;279:11882–9.

A Selective Phosphatase of Regenerating Liver Phosphatase Inhibitor Suppresses Tumor Cell Anchorage-Independent Growth by a Novel Mechanism Involving p130Cas Cleavage

Sherif Daouti, Wen-hui Li, Hong Qian, et al.

Cancer Res 2008;68:1162-1169.